SUPPLEMENTARY MATERIAL

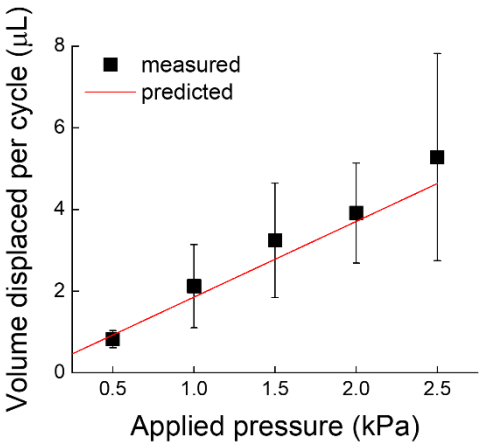

Figure S1. Fluid volume displaced in the pressure chamber of the MicroHeart as a function of pressure applied. Experimental values obtained from measurements of bead displacement in the large microfluidic channel (fluidic circuit open) are compared to the prediction by Equation 1 where the slope of the graph captures the capacitance of the pumping chamber (C_i).

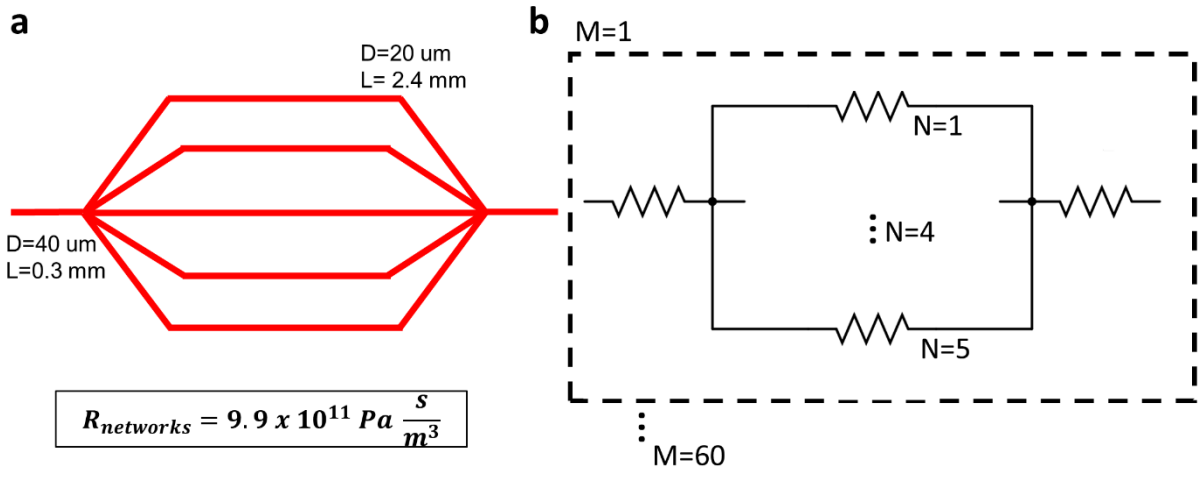

Figure S2. (a) Estimation of the hydraulic resistance of microvascular networks based on images of the microvascular networks and considering the vessel paths as a series of cylindrical, connected segments with a given length and radius. (b) Translation of the approximated geometry to a series of parallel and serial resistances. A basic circuit unit "M" was established to represent the connected hydraulic resistances with a repeating pattern of this unit to consider the total number of vessel paths of the microvascular networks that contributed to the net fluid resistance. Based on empirical comparison to experimental measurements of the total hydraulic resistance ($R_{experimental}$= 1.1 x 10^{12} Pa s /m^3), we estimated that a total of 60 repeating units of M optimally approximated the experimental value of the net hydraulic resistance ($R_{analytical}$= 9.9 x 10^{11} Pa s /m^3).

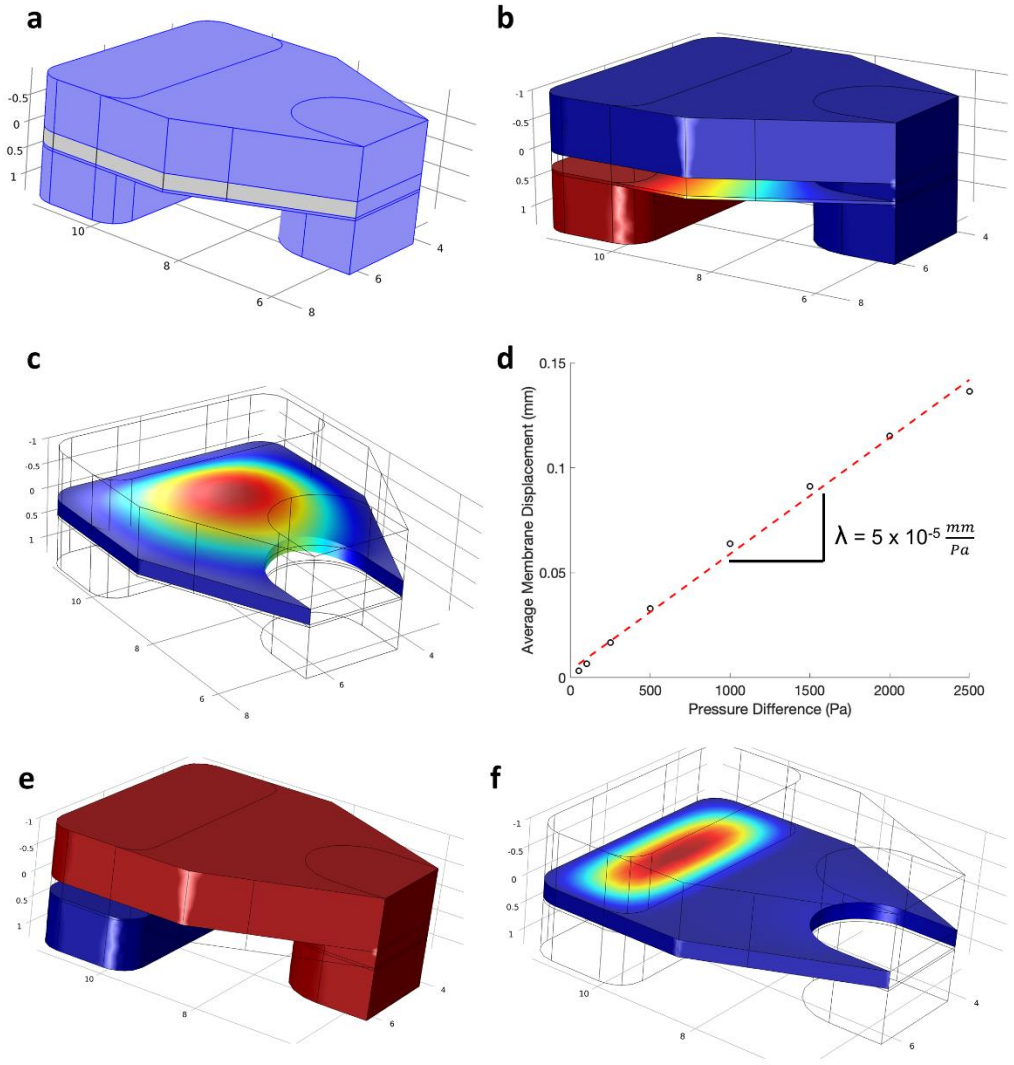

Figure S3. (a) Imported CAD of the diode to COMSOL with the membrane shown in gray and the fluid domain depicted in blue. (b) Fluid pressure difference applied across the membrane with P_{max} in red with pressure diminishing to blue corresponding to P_{min}. (c) Simulation result of the membrane deformation accordingly to the fluid pressure difference with the lowest deformation shown in blue leading up to the highest deformation as red. (d) Plotted results for the average membrane displacement as a function of pressure difference. The slope of the graph indicates the inverse plate stiffness parameter. (e) Imported CAD of the diode in COMSOL with the fluid pressure difference applied across the membrane in the reverse direction with P_{max} in red and P_{min} in blue. (f) Membrane displacement as a result of the reverse direction pressure difference with the lowest deformation shown in blue leading up to the highest deformation as red. Simulation results showed that a pressure difference in the reverse direction as low as 100 Pa impedes backflow in the check-valves. Pressure differences in the reverse direction effectively deform the membrane downwards via the membrane hole that connects the check-valve with the upstream channel, thus closing off the fluid path.

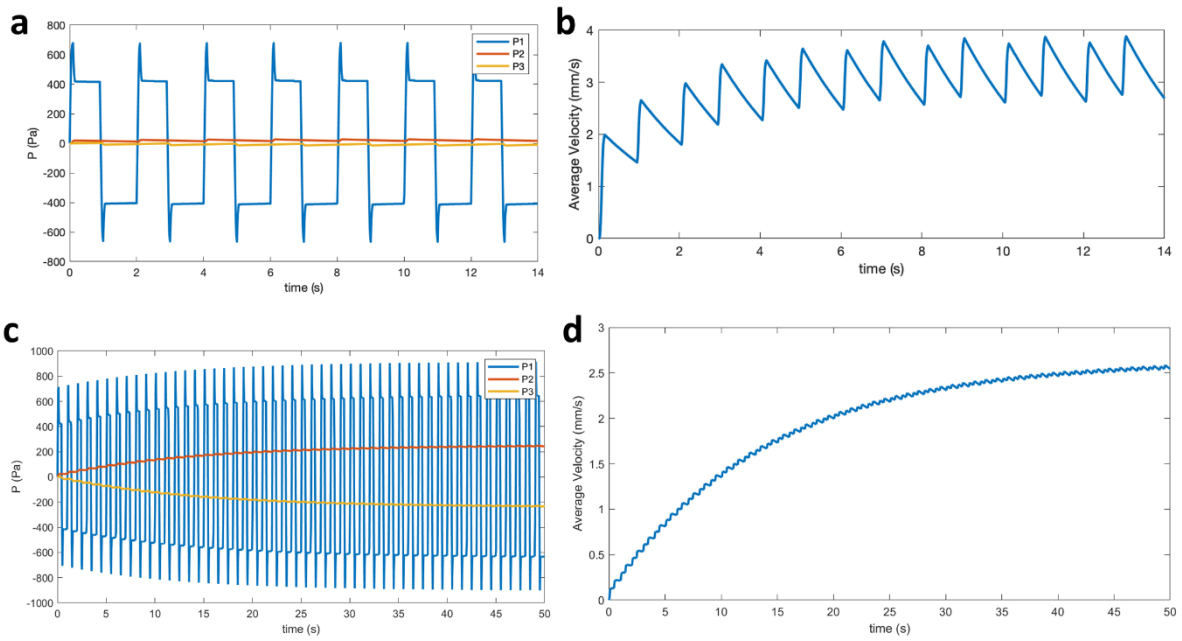

Figure S4. (a) Plot of the time-varying pressures at different nodes of the lumped parameter model circuit during pumping of the small channel-microfluidic device . (b) Average velocity plot for the fluid flow across the small channel-microfluidic device estimated from the simulation results of the lumped element model. Both plots (a-b) correspond to a pumping frequency of 2 Hz with an applied pressure of 1500 Pa. (c) Plot of the time-varying pressures at different nodes of the lumped parameter model circuit during pumping of the microvascular networks. (d) Average velocity plot for the fluid flow across the microvascular networks estimated from the simulation results of the lumped element model. Both plots (c-d) correspond to a pumping frequency of 1 Hz with an applied pressure of 1800 Pa.

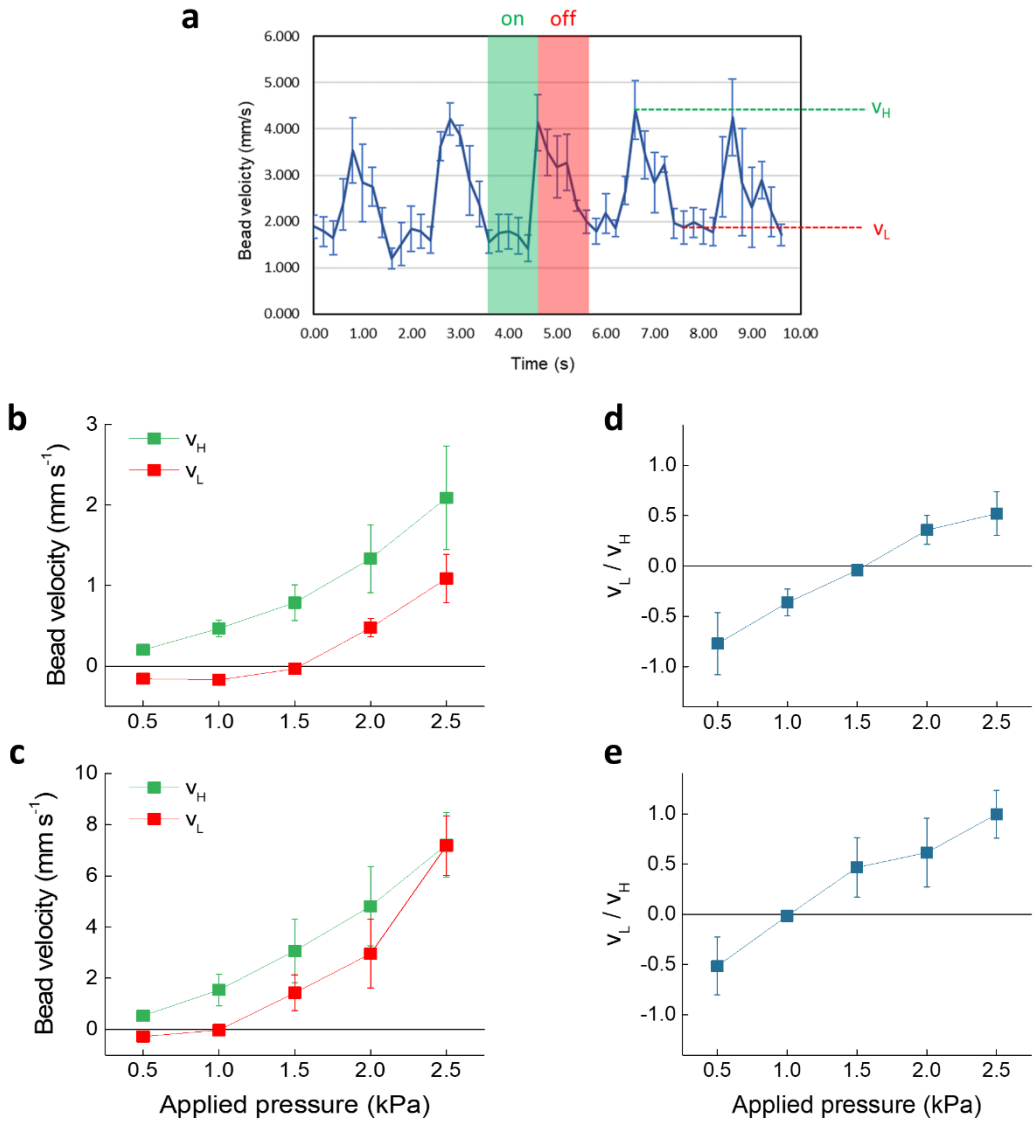

Figure S5. (a) Bead velocity over time (large microfluidic channel, 1.5 kPa, 1 Hz) and definition of v_L and v_H. Measurements of these velocities are reported in the large (b) and small (c) microfluidic channels (average and standard deviation). The corresponding ratios are reported in (d) and (e) for the large and small microfluidic channels, respectively.

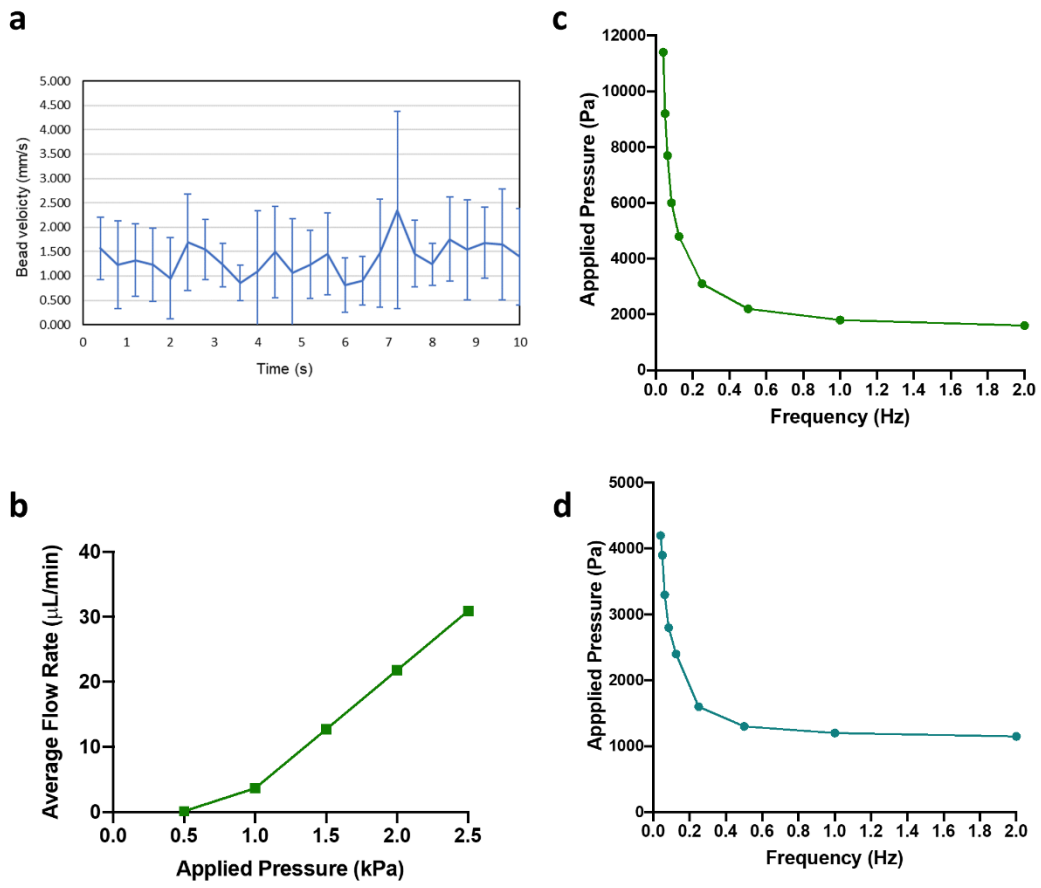

Figure S6. (a) Bead velocity as a function of time in the microvascular networks (1.5 kPa, 1 Hz, average and standard deviation reported). (b) Computational model prediction of net flow rate in the networks as a function of pressure at a frequency of 1 Hz. The model prediction for applied pressure and frequency pairs required to exert an endothelial shear stress of 1 Pa in microvascular networks are reported for (c) a 3 mm-wide channel and (d) a 1.2 mm-wide channel devices.

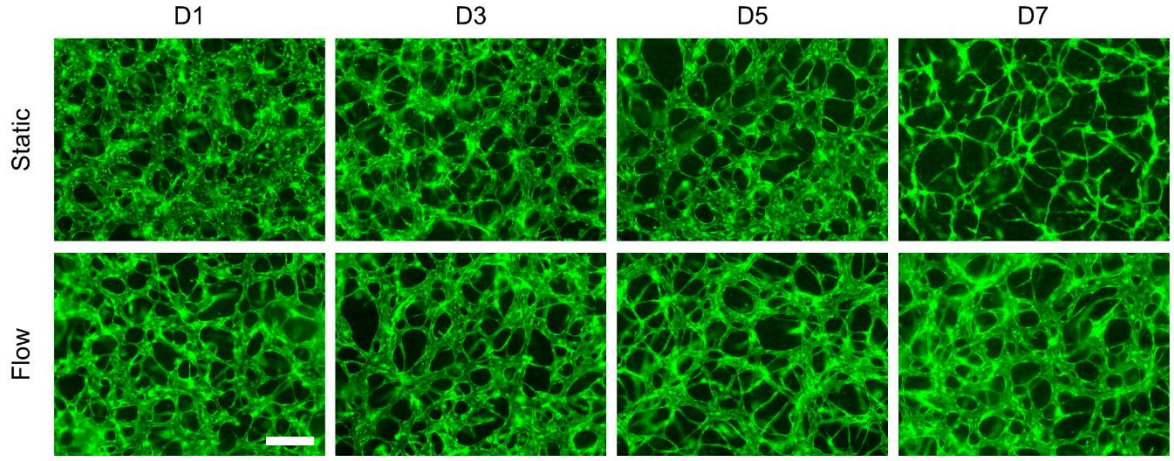

Figure S7. Representative fluorescence microscopy images of microvascular networks (green – GFP signal) under static or MicroHeart flow conditions over 7 days. The scale bar is 200 μm.

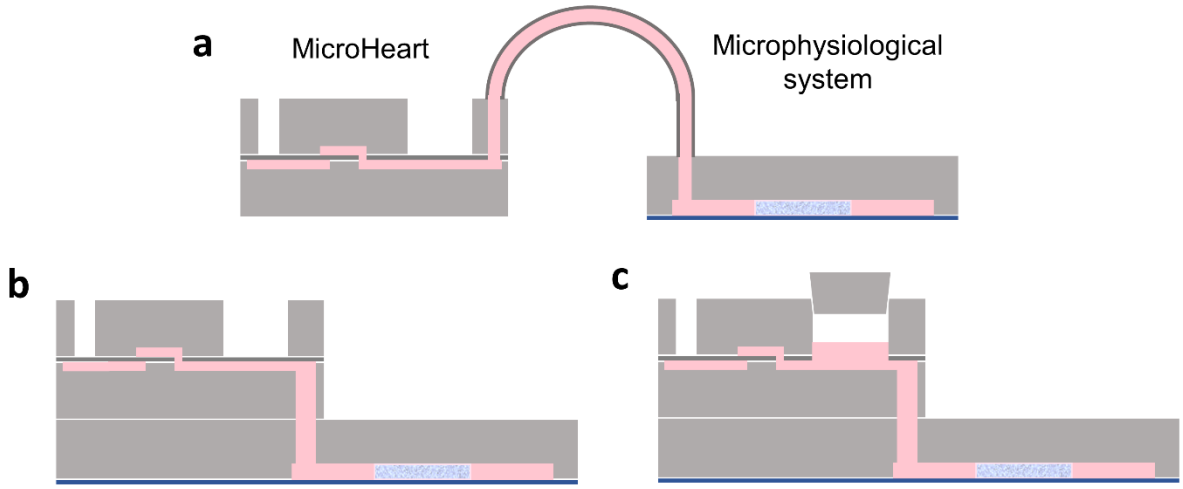

Figure S8. (a) Cross sectional view of the MicroHeart connected to a microfluidic device as presented in this paper. Two alternatives to the MicroHeart design are presented: (b) eliminating the tubing and placing the MicroHeart directly on top of a microfluidic device, and (c) building from (b) by using an air spring as the basis for the capacitor rather than the currently proposed deflecting silicone membrane. The air spring capacitor may feature a removable plug which can be used for media sampling and changing. Using an isothermal process assumption and capacitor dimensions of 9 mm diameter and 5 mm height, 0.94 µL of liquid medium would need to fill the capacitor space to achieve a pressure of 300 Pa.

Video S1. Real-time video of fluorescent beads flowing through a microvascular network under 2.5 kPa and 1 Hz MicroHeart flow. The dimensions are the same as in Figure 3a.